Theoretical Calculations and Infrared Absorption Spectra of *ap*- and *sp*-Methyl Vinyl Ketone in Solid Ar

K. Sankaran and Yuan-Pern Lee*

Department of Chemistry, National Tsing Hua University, 101, Sec. 2, Kuang Fu Road, Hsinchu, Taiwan 30013

Received: August 30, 2001; In Final Form: November 27, 2001

Infrared absorption spectra of methyl vinyl ketone (MVK, butenone) isolated in solid Ar were recorded. Irradiation of MVK at 308 nm partially converts antiperiplanar (*ap*-, previously called *s-trans*) MVK to synperiplanar (*sp*-, previously called *s-cis*) MVK; the difference spectrum clearly distinguishes absorption lines of these two conformers. Calculations using density functional theories (B3LYP with an aug-cc-pVTZ basis set) were performed to predict the geometry, energy, vibrational wavenumbers, and infrared intensities of *ap*- and *sp*-MVK. Experimental results on vibrational wavenumbers and relative intensities agree with theoretical calculations. To distinguish these conformers isolated in matrices, irradiation in situ is more effective than use of supersonic expansion during deposition.

Introduction

Spectra of conformers of α, β-unsaturated carbonyl compounds and their application to investigation of equilibrium between conformers have commanded much attention.[1] For these compounds that serve as dieneophiles in the Diels−Alder reaction, the conformational equilibrium can have effects on the selectivity and reactivity of the reaction.

Methyl vinyl ketone (or butanone, designated as MVK hereafter) is the simplest α, β-unsaturated ketone. It was demonstrated recently that MVK is a useful precursor of vinyl radicals,[2,3] but spectra of conformers of MVK are poorly characterized.[1,4−10] Although intense absorption lines near 1700 cm^{-1} associated with C═O bond-stretching motion for the two conformers, antiperiplanar (*ap*-, previously called *s-trans*) and synperiplanar (*sp*-, previously called *s-cis*) MVK, are well characterized, no other lines with wavenumbers greater than 1400 cm^{-1} are distinguished between these two conformers. Initial assignments of some lines were made by Durig and Little[8] and by Oelichmann et al.;[10] de Smedt et al. revised the assignments based on analysis of microwave and IR spectra, data from electron diffraction in the gas phase, and quantum-chemical calculations at a 4-21G level.[1] Earlier experiments on the temperature dependence of features in IR spectra led to assignments of low-frequency spectral lines of *ap*-MVK and *sp*-MVK, upon which an equilibrium for conversion between these conformers was established.[5−8] *ap*-MVK is more stable than *sp*-MVK by 0.6−0.8 kcal mol^{-1}, with a barrier of ∼1.4 kcal mol^{-1} for conversion from *ap*-MVK to *sp*-MVK.[5,7,8]

Quantum-chemical calculations,[1,11,12] yielded geometries and energies of conformers of MVK; the energy difference between *ap*- and *sp*-MVK varies with method, but a calculation with MP3/6-311++G** and geometry optimized with the RHF/6-311++G** method predicted that *ap*-MVK is more stable than *sp*-MVK by 0.5 kcal mol^{-1},[11] consistent with experiments. de Smedt et al. reported calculated vibrational wavenumbers for both conformers[1] but made conformational assignments of observed lines to only 15 vibrational modes; 12 additional lines, mostly above 1300 cm^{-1}, were assigned to both conformers.

Krantz et al. irradiated MVK isolated in solid Ar with light from a medium-pressure mercury arc, filtered through a solution of nickel sulfate, for 4 h and observed partial conversion from *ap*-MVK to *sp*-MVK.[9] They assigned lines only below 1750 cm^{-1}. Parker and Davis[13] observed formation of MVK from photochemical reaction of O_3 with dimethylacetylene (butyne-2) in solid Ar, but neither identified lines above 1750 cm^{-1} nor made conformational assignments.

By observing the difference spectrum after irradiation with light from a laser, we have readily identified IR lines associated with *sp*- and *ap*-MVK. Here we report experimental identification of both conformers of MVK in matrices according to such a technique with results from quantum-chemical calculations.

Experimental Section

The experimental setup is similar to that described previously.[14,15] Matrix samples were prepared on co-depositing MVK and Ar in a mixture, with a volumetric ratio typically in a range 1/500 to 1/5000 onto a platinum-plated copper mirror maintained at 13 K; deposition was performed either via an effusive beam or via supersonic expansion. Approximately 10 mmol of mixture was deposited over a period of 2−3 h.

A Nd:YAG laser (1.06 μm and 532 nm), a XeCl excimer laser (308 nm), and an ArF excimer laser (193 nm) were employed to irradiate MVK isolated in solid Ar; a repetition rate of 10 Hz and an energy ∼5 mJ were typically employed. After each stage of irradiation, IR absorption spectra were recorded with an FTIR spectrometer equipped with a KBr beam splitter and a Hg−Cd−Te detector (77 K). Typically 500 scans were collected at a resolution of 0.5 cm^{-1}.

MVK (>95%, Tokyo Kasei Organic Chemicals) was used without further purification except degassing at 77 K. Ar (99.9995%, AGA Specialty Gases) was used without purification.

Computational Method. The equilibrium structure, vibrational wavenumbers, IR intensities, and energies were calculated with the Gaussian 98 program.[16] We used Hartree−Fock (HF)

* To whom correspondence should be addressed. Jointly appointed by the Institute of Atomic and Molecular Sciences, Academia Sinica, Taipei, Taiwan. E-mail: yplee@mx.nthu.edu.tw.

10.1021/jp013362h CCC: $22.00 © 2002 American Chemical Society
Published on Web 01/30/2002

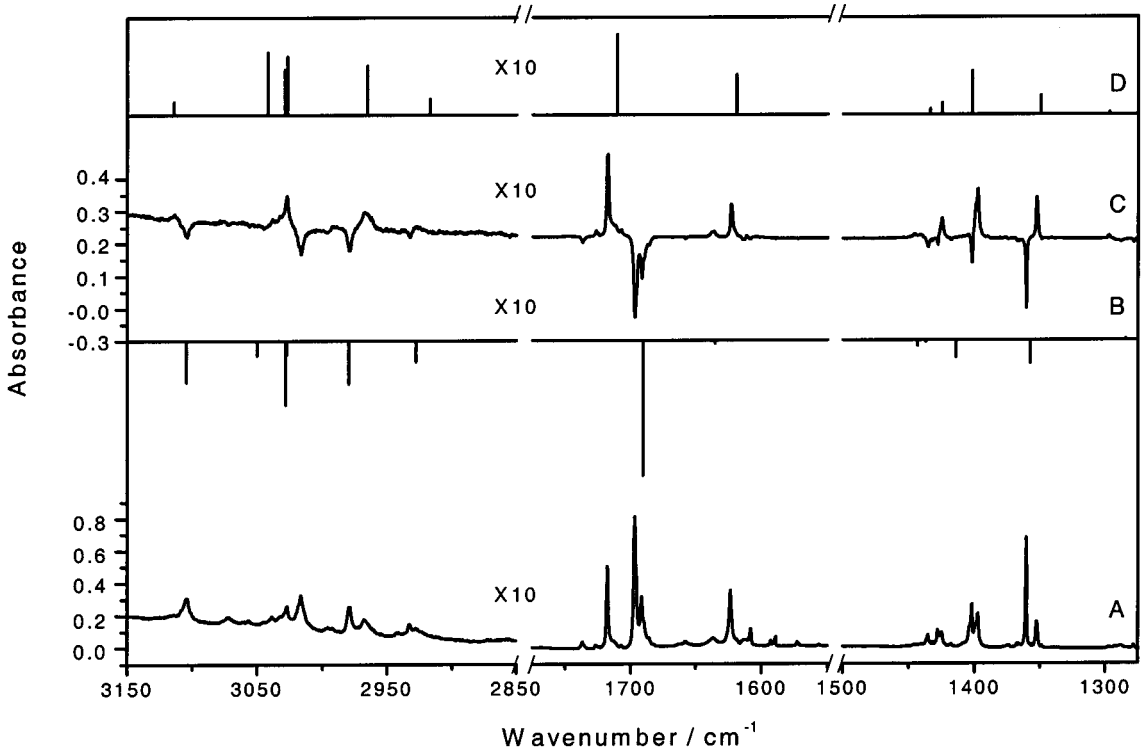

Figure 1. Spectra of MVK in regions 3150−2850, 1775−1550, and 1500−1275 cm^{-1} (A) MVK/Ar = 1/800 at 13 K after deposition; (B) theoretically predicted (inverted) line spectrum of *ap*-MVK; (C) difference spectrum of the matrix sample after irradiation at 308 nm for 2.5 h; (D) theoretically predicted line spectrum of *sp*-MVK.

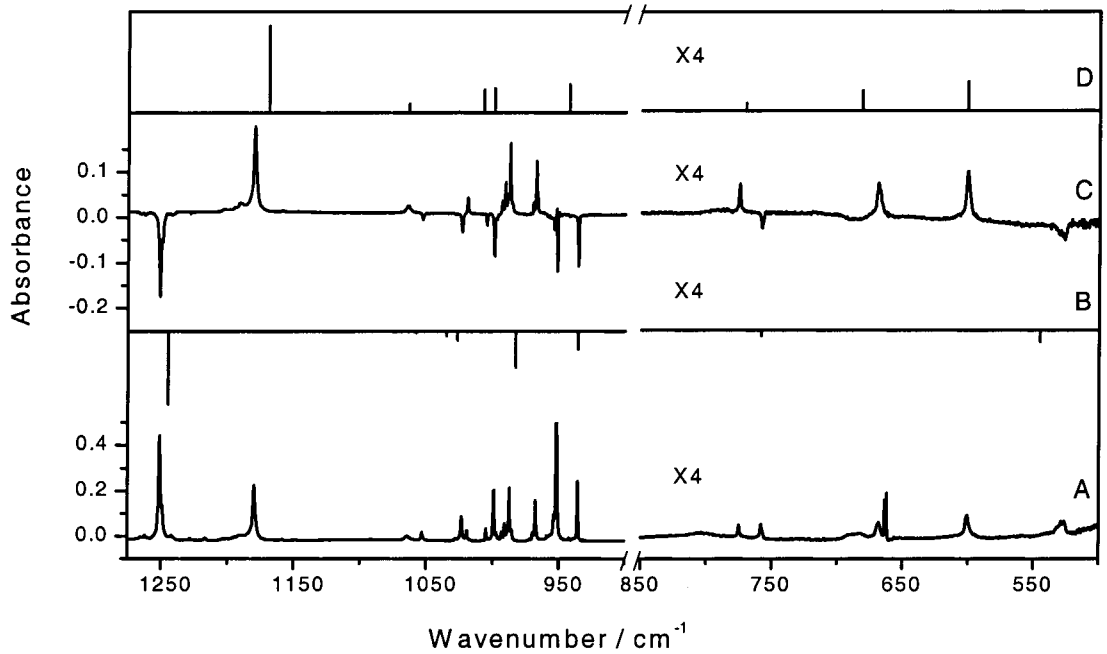

Figure 2. Spectra of MVK in regions 1275−900 and 850−500 cm^{-1} (A) MVK/Ar = 1/800 at 13 K after deposition; (B) theoretically predicted (inverted) line spectrum of *ap*-MVK; (C) difference spectrum of the matrix sample after irradiation at 308 nm for 2.5 h; (D) theoretically predicted line spectrum of *sp*-MVK.

and B3LYP density functional theory (DFT) with 6-31G** and Dunning's correlation-consistent polarized valence triplet-zeta basis set, augmented with s, p, d, and f functions (aug-cc-pVTZ).[17] The B3LYP method uses Becke's three-parameter hybrid exchange functional, which includes the Slater exchange functional with corrections involving a gradient of the density, and a correlation functional of Lee, Yang, and Parr, with both local and nonlocal terms.[18,19] Analytic first derivatives were utilized in geometry optimization, and vibrational frequencies were calculated analytically at each stationary point.

Results and Discussion

A. Irradiation of MVK in Solid Ar. Partial IR spectra of a matrix sample deposited from an effusive beam of MVK in Ar (1/800) appear in traces A in both Figure 1 for spectral ranges 3150−2850, 1775−1550, and 1500−1275 cm^{-1} and Figure 2

TABLE 1: Comparison of Calculated and Experimental Results for Vibrational Wavenumbers (in cm^{-1}) of *ap*-MVK

calculation			experiments			
4-21G ref 1	B3LYP/aug-cc-pVTZ this work	scaled[a]	Ar matrix this work	Ar matrix ref 9	gas phase[b] ref 8	approximate assignments
3089	3223.2 (6.4)[c]	3104.5	3104.5 (4.5)[d]		(3105)[e]	CH_2 asym str
3053	3166.0 (2.3)	3050.0	3056.3 (0.3)		(3036)	CH str
3018	3143.0 (9.9)	3028.1	3015.8 (5.0)		(3019)	CH_2 sym str
3012	3142.1 (2.2)	3027.2	3015.8 (5.0)		(2996)	CH_3 asym str
2969	3092.1 (6.7)	2979.5	2979.1 (3.6)		(2971)	CH_3 asym str
2913	3037.7 (3.3)	2927.7	2932.6 (0.8)		(2936)	CH_3 sym str
1716	1739.4 (208)	1690.5	1696.1 (208) 1691.1	1690	1705	CO str
1657	1681.6 (5.4)	1635.5	1657.8 (8.3)		(1620)	C═C str
1436	1480.2 (9.4)	1443.5	1435.5 (8.1)		(1437)	CH_3 asym def
1426	1474.0 (3.3)	1437.6	1427.6 (3.8)		(1426)	CH_3 asym def
1402	1449.5 (27.2)	1414.3	1402.0 (34.9)		(1400)	CH_2 sym def
1355	1390.1 (36.5)	1357.7	1360.6 (53.5)	1355	(1355)	CH_3 sym def
1278	1313.2 (2.1)	1284.4	1278.1 (2.5)		1283	HC═C bend
1256	1271.4 (80.6)	1244.6	1250.9 (78.4)	1250	1249	CC(O)C asym str
1047	1075.7 (2.4)	1058.3	1053.4 (3.4)	1051	(1108)	CH_2 rock
1023	1051.7 (5.6)	1035.2	1023.1 (10.2)	1021	(1026)	CH_3 twisting
993	1043.1 (10.3)	1027.0	1005.1 (3.2)	1003	1002	C═C torsion
936	996.8 (40.0)	982.9	999.0 (23.1) 951.3 (65.0)	997 950	987	CH_2 wag
907	947.4 (19.8)	935.8	935.6 (18.2)		950	CH_3 rock
759	761.0 (2.5)	758.2	758.2 (3.1)	756	758	CC(O)C sym def
726	700.2 (5.8)	700.3		616	691	out-of-plane def
546	537.9 (5.3)	545.6	526.7? (7.2)[f]		530	in-plane def
486	493.0 (9.3)				492	in-plane def
425	433.3 (0.3)				413	out-of-plane def
281	277.6 (2.9)				292	in-plane def
150	130.1 (0.4)				125	mixed torsion
117	114.4 (1.4)				116	mixed torsion

[a] $(3104.5 - \nu_{scaled})/(\nu_{scaled} - 758.2) = (3223.2 - \nu_{calc})/(\nu_{calc} - 761.0)$. [b] The assignments were revised by de Smedt et al.[1] [c] Predicted IR intensities in km mol^{-1} are listed in parentheses. [d] Relative intensities of observed lines with the intensity of the most intense line at 1696.1 cm^{-1} set to the calculated value. [e] Wavenumbers in parentheses were assigned to both *ap*- and *sp*-MVK. [f] This line was not used as a reference of scaling because of its broad width and uncertainty in wavenumbers.

for ranges 1275−900 and 850−500 cm^{-1}. Irradiation of the matrix sample with laser emission at 532 nm, 1.06 μm, or emission from the globar source of the spectrometer for more than 2 h produced no alteration of the spectrum. Irradiation of the sample with laser emission at 308 nm alters relative intensities of observed lines, but produces no new lines. Trace C in both Figures 1 and 2 is a difference spectrum after irradiation of the sample for 2 h. The difference spectra are derived on subtracting spectra before irradiation from those recorded after irradiation; lines pointing upward indicate production after irradiation, whereas those pointing downward indicate destruction. Experiments with varied concentrations and periods of irradiation show that all lines pointing upward belong to one group, designated group "*c*", and those pointing downward belong to another group, designated group "*t*". Observed wavenumbers for lines in groups *t* and *c* are listed in Tables 1 and 2, respectively.

Irradiation of the matrix sample at 193 nm for 30 min produces similar results with partial conversion of lines in group *t* to group *c*, but further irradiation diminishes lines in both groups and produces new lines ascribable to C_2H_2 (3287, 3260, and 737 cm^{-1}),[20] CH_4 (3034 and 1304 cm^{-1}),[21] propylene (3090, 2981, 2940, 2922, 1453, 1440, and 910 cm^{-1}),[22] propyne (3333 and 631 cm^{-1}), [22] and some unidentified species. Laser emission at 308 nm is hence preferable to effect photoconversion between conformers of MVK.

B. Theoretical Calculations. *1. Geometry and Energy.* Theoretical calculations (HF and B3LYP) indicate two stable isomers of MVK, *ap*-MVK and *sp*-MVK, as illustrated in Figure 3. Both HF/6-31G** and B3LYP/6-31G** methods predict that *sp*-MVK is more stable than *ap*-MVK by ∼0.3 kcal mol^{-1} after correction for vibrational zero-point energy (ZPE). In contrast, the B3LYP/aug-cc-pVTZ method predicts *ap*-MVK to be more stable by 0.13 kcal mol^{-1} after correction of ZPE. Garcia et al. also reported a similar trend,[11] with energy of *ap*-MVK less than that of *sp*-MVK by ∼0.5 kcal mol^{-1} at the MP3/6-311++G** level of calculation. Our predicted geometry and energy of each isomer are listed in Table 3 and compared with previous results. Structures predicted with various theoretical methods agree satisfactorily. The absolute energy predicted with B3LYP/aug-cc-pVTZ is less than that with MP3/6-311++G**, but relative energy of two conformers is within error of calculation.

2. Vibrational Wavenumbers and Mode Assignments. Vibrational wavenumbers and infrared intensities of *ap*-MVK and *sp*-MVK predicted with B3LYP/aug-cc-pVTZ are listed in Tables 1 and 2 for comparison with experiments and previous calculations. Variations in wavenumbers for lines above 600 cm^{-1} for *ap*-MVK and *sp*-MVK are within 5%, with average deviations 2.9 ± 1.2% and 2.6 ± 1.1%, respectively. After a linear scaling to match observed wavenumbers of lines with the greatest and least wavenumbers in an Ar matrix, the maximum deviation decreased to 4%, with average deviations 0.8 ± 1.1% and 0.6 ± 0.7% for *ap*-MVK and *sp*-MVK, respectively; most observed lines are within 10 cm^{-1} of scaled predictions. Prediction of vibrational wavenumbers using B3LYP is superior to that with the 4-21G method.

Calculated relative IR intensities also agree satisfactorily with experimental observations, as listed in parentheses in columns 2 and 4 of Tables 1 and 2. Traces B and D of Figures 1 and 2

TABLE 2: Comparison of Calculated and Experimental Results on Vibrational Wavenumber (in cm^{-1}) of *sp*-MVK

calculation			experiments			
4-21G ref 1	B3LYP/aug-cc-pVTZ this work	scaled[a]	Ar matrix this work	Ar matrix ref 9	gas phase[b] ref 8	approximate assignments
3102	3232.2 (1.9)[c]	3113.9	3113.9 (0.2)[d]		(3105)[e]	CH_2 asym str
3052	3156.6 (9.6)	3041.7	3038.6 (0.7)		(3036)	CH str
3020	3142.8 (7.0)	3028.5	3026.9 (2.4)		(3019)	CH_3 asym str
3017	3140.7 (9.0)	3026.5	2991.7 (0.3)		(2996)	CH_2 sym str
2959	3076.4 (7.6)	2965.1	2967.3 (4.2)		(2971)	CH_3 asym str
2908	3026.1 (2.4)	2917.0	2926.6 (0.4)		(2936)	CH_3 sym str
1721	1763.2 (123.7)	1710.6	1717.6 (123.7)	1710	1729	CO str
1649	1667.7 (61.5)	1619.3	1623.3 (107.3)		(1620)	C═C str
1428	1473.6 (8.3)	1433.9	1445.9 (1.7)		(1437)	CH_3 asym def
1416	1464.3 (17.2)	1425.0	1424.5 (12.2)		(1426)	CH_3 asym def
1391	1439.9 (66.3)	1401.7	1396.7 (42.1)		(1400)	CH_2 sym def
1352	1385.2 (28.1)	1349.5	1352.0 (29.6)	1348	(1355)	CH_3 sym def
1288	1330.2 (2.8)	1296.9	1297.9 (1.8)	1293	1298	HC═C bend
1211	1196.3 (94.0)	1169.0	1179.5 (104.9)	1179	1218	CC(O)C asym str
1058	1086.1 (9.4)	1063.7	1064.3 (6.4)	1061	(1108)	CH_2 rock
1033	1047.3 (0.5)	1026.7	1019.2 (4.5)	1018	(1026)	CH_3 twisting
1017	1026.9 (24.7)	1007.2	993.0 (3.2)		1002	C═C torsion
			990.8 (4.9)			
994	1018.7 (26.4)	999.4	987.0 (32.7)	989	987	CH_2 wag
960	959.7 (30.5)	943.0	967.2 (25.2)	966	968	CH_3 rock
784	778.8 (3.4)	770.2	774.6 (3.0)	773	772	CC(O)C sym def
676	686.0 (8.9)	681.6	668.0 (8.2)		662	out-of-plane def
620	601.7 (13.1)	601.0	601.0 (20.9)	603	609	in-plane def
444	459.1 (0.3)				492	out-of-plane def
424	415.9 (3.8)				422	in-plane def
270	268.8 (4.4)				272	in-plane def
125	118.5 (0.0)				121	$(H_3)C-C(O)$ torsion
107	87.2 (0.9)				87	(C═)C−C(O) torsion

[a] $(3113.9 - \nu_{scaled})/(\nu_{scaled} - 601.0) = (3232.2 - \nu_{calc})/(\nu_{calc} - 601.7)$. [b] The assignments were revised by de Smedt et al.[1] [c] Predicted IR intensities in km mol^{-1} are listed in parentheses. [d] Relative intensities of observed lines with the intensity of the most intense line at 1717.6 cm^{-1} set to the calculated value. [e] Wavenumbers in parentheses were assigned to both *ap*- and *sp*-MVK.

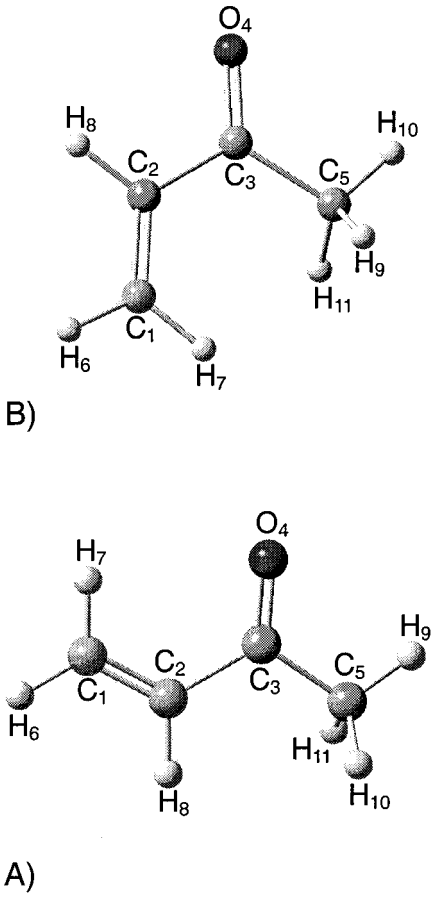

Figure 3. Geometries of conformers *sp*-MVK (A) and *ap*-MVK (B) calculated with the B3LYP/aug-cc-pVTZ method.

depict theoretically predicted line spectra (after scaling) of *ap*-MVK and *sp*-MVK, respectively, for comparison with difference spectra in trace C; trace B is inverted for convenience in comparison with the downward lines of *ap*-MVK. Predicted and observed spectra thus agree satisfactorily.

For *ap*-MVK, an extra line at 1691.1 cm^{-1} might be assigned to a combination band of lines at 982.9 and 700.3 cm^{-1}. A line predicted at 982.9 cm^{-1} splits into a doublet at 999.0 and 951.3 cm^{-1}, likely reflecting its Fermi resonance with the overtone of a line at 493.0 cm^{-1}. For *sp*-MVK, a line predicted at 943.0 cm^{-1} is observed at 967.2 cm^{-1}; there is no obvious combination or overtone bands in this region, and such a large error for only this line between theory and experiment is inexplicable.

3. Barrier for Conversion from ap-MVK to sp-MVK. With B3LYP/aug-cc-pVTZ, a transition state for conversion between *ap*-MVK and *sp*-MVK is located with a CCCO torsional angle near 90°; the geometry and energy of this transitional state is also listed in Table 3. After correction for vibrational zero-point energy, a barrier of 4.87 kcal mol^{-1} is derived for conversion from *sp*-MVK to *ap*-MVK; the barrier for the reverse reaction is 5.00 kcal mol^{-1}. The barrier in an Ar matrix is expected to be greater than the value predicted for a species in the gas phase. The relatively large barrier can explain why irradiation of the matrix sample with an IR source fails to induce the conformational change.

C. Comparison of Efficiency in Conformational Conversion Between Use of Supersonic Expansion and Use of Laser Radiation. It has been demonstrated that relative populations of conformers at ambient temperature can be altered on use of a supersonic expansion for deposition.[23,24] To investigate the effect of supersonic expansion, we probed the ratio, designated as I_{ap}/I_{sp}, of intensity of a line at 1696.1 cm^{-1} for *ap*-MVK to

TABLE 3: Geometries[a] and Energies of Two Conformers and Transition States (TS) of MVK Predicted with Various Theoretical Methods[c]

	sp-MVK		*ap*-MVK		TS
parameters	de Smedt	this work	de Smedt	this work	this work
$r(C_1C_2)$	1.314	1.329	1.314	1.331	1.325
$r(C_2C_3)$	1.501	1.494	1.498	1.485	1.504
$r(O_4C_3)$	1.189	1.214	1.189	1.216	1.210
$r(C_5C_3)$	1.518	1.511	1.521	1.514	1.510
$r(H_6C_1)$	1.077	1.081	1.077	1.082	1.082
$r(H_7C_1)$	1.077	1.082	1.077	1.082	1.083
$r(H_8C_2)$	1.078	1.084	1.078	1.083	1.086
$r(H_9C_5)$	1.082	1.086	1.082	1.086	1.087
$r(H_{10}C_5)$	1.088	1.093	1.087	1.091	1.092
$r(H_{11}C_5)$	1.088	1.093	1.087	1.091	1.092
$\angle C_1C_2C_3$	119.8	122.0	125.2	125.4	124.2
$\angle O_4C_3C_2$	121.8	122.0	119.8	119.3	120.9
$\angle C_5C_3C_2$	115.8	116.1	118.5	119.6	116.6
$\angle H_6C_1C_2$	119.6	121.8	122.6	121.3	121.4
$\angle H_7C_1C_2$	122.5	120.2	121.3	122.3	121.8
$\angle H_8C_2C_1$	122.1	120.8	121.3	120.9	120.7
$\angle H_9C_5C_3$	109.6	110.2	108.3	108.9	110.4
$\angle H_{10}C_5C_3$	109.9	110.1	110.5	110.8	110.1
$\angle H_{11}C_5C_3$	109.9	110.1	110.5	110.8	109.6
$\varphi O_4C_3C_2C_1$	0.0	0.0	180.0	180.0	90.5
$\varphi C_5C_3C_2C_4$		180.0		0.0	178.9
$\varphi H_6C_1C_2C_3$		180.0		180.0	−178.2
$\varphi H_7C_1C_2H_6$		180.0		180.0	179.1
$\varphi H_8C_2C_1H_7$		180.0		180.0	179.7
$\varphi H_9C_5C_3O_4$	0.0	0.0	0.0	0.0	3.4
$\varphi H_{10}C_5C_3H_9$		121.3		120.4	121.9
$\varphi H_{11}C_5C_3H_9$		−121.3		−120.4	−121.4
E/hartree	−229.4236	−231.329001	−229.4217	−231.329476	−231.320509
ZPE/hartree		0.088962		0.089224	0.088219
E_{rel}[b]/kcal mol^{-1}	0.0	0.13	1.17	0.00	5.00

[a] Bond lengths are in Å and angles are in degrees. [b] Zero-point energy (ZPE) corrected energy relative to the lowest value. [c] MP3/6-311++G** (ref 11) yields $E_{rel} = 0.5$ kcal mol^{-1} for *sp*-MVK relative to *ap*-MVK.

that at 1717.6 cm^{-1} for *sp*-MVK. With an effusive beam, $I_{ap}/I_{sp} = 2.90$, whereas I_{ap}/I_{sp} increases to 2.94 for supersonic expansion with a stagnation pressure of 1000 Torr. Further increase of stagnation pressure to 3000 Torr increases slightly this ratio to $I_{ap}/I_{sp} = 3.11$. Compared with the extent of conversion using laser irradiation, which produced $I_{ap}/I_{sp} = 1.13$, such a variation in relative population of conformers is marginal. Furthermore, the line shape varies with deposition conditions, leading to difference spectra of poorer quality. We find that photoconversion is superior to supersonic expansion for identification of spectral lines of various conformers of MVK.

Supersonic expansion provides an advantage that the more stable conformer is expected to gain more population at low temperature; the expansion experiments clearly indicate that *ap*-MVK is more stable than *sp*-MVK, consistent with previous experimental work and more sophisticated calculations.

Conclusion

Irradiation of MVK in solid Ar with laser emission at 308 nm partially converts *ap*-MVK to *sp*-MVK to enable us to identify all IR absorption lines of *ap*-MVK and *sp*-MVK for the first time. Observed wavenumbers agree satisfactorily with theoretical calculations using the B3LYP/aug-cc-pVTZ method. The conformer *ap*-MVK is 0.13 kcal mol^{-1} more stable than *sp*-MVK with a barrier ∼5 kcal mol^{-1} for conversion from *ap*-MVK to *sp*-MVK. To distinguish the two conformers of MVK, irradiation proved superior to supersonic expansion.

Acknowledgment. We thank the National Science Council of Taiwan, the Republic of China (grant no. NSC90-2119-M-007-050) for support.

References and Notes

(1) de Smedt, J.; Vanhouteghem, F.; van Alsenoy, C.; Geise, H. J.; van der Veken, B.; Coppens, P. *J. Mol. Struct.* **1989**, *195* 227.
(2) Pibel, C. D.; McIlroy, A.; Taatjes, C. A.; Alfred, S.; Patrick, K.; Halpern, J. B. *J. Chem. Phys.* **1999**, *110*, 1841.
(3) Letendre, L.; Liu, D.-K.; Pibel, C. D.; Halpern, J. B.; Dai, H. L. *J. Chem. Phys.* **2000**, *112*, 9209.
(4) Foster, P. D.; Rao, V. M.; Curl, R. F., Jr. *J. Chem. Phys.* **1965**, *43*, 1064.
(5) Pentin, Y. A. *J. Mol. Struct*. **1978**, *46*, 149.
(6) Noack, K.; Jones, R. N. *Can. J. Chem*. **1961**, *39*, 2225.
(7) Bowles, A. J.; George, W. O.; Maddams, W. F. *J. Chem. Soc. B* **1969**, 810.
(8) Durig, J. R.; Little, T. S. *J. Chem. Phys.* **1981**, *75*, 3660.
(9) Krantz, A.; Goldfarb, T. D.; Lin, C. Y. *J. Am. Chem. Soc*. **1972**, *94*, 4022.
(10) Oelichmann, H. J.; Bougeard, D.; Schrader, B. *J. Mol. Struct.* **1981**, *77*, 179.
(11) Garcia, J. I.; Mayoral, J. A.; Salvatella, L.; Assfeld, X.; Ruiz-Lopez, M. F. *J. Mol. Struct*. (*Theochem*) **1996**, *362*, 187.
(12) Jorgensen, W. L.; Lim, D.; Blake, J. F. *J. Am. Chem. Soc.* **1993**, *115*, 2936.
(13) Parker, J. K.; Davis, S. R. *J. Phys. Chem. A* **1999**, *103*, 7280.
(14) Kuo, Y.-P.; Wann, G.-H.; Lee, Y.-P. *J. Chem. Phys.* **1993**, *99*, 3272.
(15) Bahou, M.; Chen, S.-F.; Lee, Y.-P. *J. Phys. Chem. A* **2000**, *104*, 3613.
(16) Frisch, M. J.; Trucks, G. W.; Schlegel, H. B.; Scuseria, G. E.; Robb, M. A.; Cheeseman, J. R.; Zakrzewski, V. G.; Montgomery, J. A. Jr.; Stratmann, R. E.; Burant, J. C.; Dapprich, S.; Millam, J. M.; Daniels, A. D.; Kudin, K. N.; Strain, M. C.; Farkas, O.; Tomasi, J.; Barone, V.; Cossi, M.; Cammi, R.; Mennucci, B.; Pomelli, C.; Adamo, C.; Clifford, S.; Ochterski, J.; Petersson, G. A.; Ayala, P. Y.; Cui, Q.; Morokuma, K.; Malick, D. K.; Rabuck, A. D.; Raghavachari, K.; Foresman, J. B.; Cioslowski, J.; Ortiz, J. V.; Baboul, A. G.; Stefanov, B. B.; Liu, G.; Liashenko, A.; Piskorz, P.; Komaromi, I.; Gomperts, R.; Martin, R. L.; Fox, D. J.; Keith, T.; Al-Laham, M. A.; Peng, C. Y.; Nanayakkara, A.; Gonzalez, C.; Challacombe, M.; Gill, P. M. W.; Johnson, B.; Chen, W.; Wong, M. W.; Andres, J. L.; Gonzalez, C.; Head-Gordon, M.; Replogle, E. S.; Pople, J. A. *Gaussian 98* (Revision A. 1); Gaussian, Inc.: Pittsburgh, PA, 1998.

(17) Dunning, T. H. *J. Chem. Phys.* **1989**, *90*, 1007.
(18) Becke, A. D. *J. Chem. Phys.* **1993**, *98*, 5648.
(19) Lee, C.; Yang, W.; Parr, R. G. *Phys. Rev.* **1988**, *B 37*, 785.
(20) Andrews, L.; Johnson, G. L.; Kelsall, B. J. *J. Phys. Chem.* **1982**, *86*, 3374.
(21) Johnson, G.; Andrews, L. *J. Am. Chem. Soc.* **1980**, *102*, 5736.
(22) Guillary, W. A.; Thomas, S. G., Jr. *J. Phys. Chem.* **1975**, *79*, 692.
(23) Vidya, V.; Sankaran, K.; Viswanathan, K. S. *Chem. Phys. Lett.* **1996**, *258*, 113.
(24) Kudoh, S.; Takayanagi, M.; Nakata, M. *Chem. Phys. Lett*. **1998**, *296*, 329.